

Origin of the literature discrepancies in the fractional reduction of the apex-field enhancement factor considering small clusters of field emitters

Thiago A. de Assis^{1,*} and Fernando F. Dall'Agnol²

¹*Instituto de Física, Universidade Federal da Bahia, Campus Universitário da Federação,
Rua Barão de Jeremoabo s/n, 40170-115, Salvador, BA, Brazil*

²*Department of Exact Sciences and Education (CEE),
Universidade Federal de Santa Catarina, Campus Blumenau,
Rua Pomerode 710 Salto do Norte, Blumenau 89065-300, SC, Brazil[†]*

Numerical simulations are important when assessing the many characteristics of field emission related phenomena. In small simulation domains, the electrostatic effect from the boundaries is known to influence the calculated apex field enhancement factor (FEF) of the emitter, but no established dependence has been reported at present. In this work, we report the dependence of the lateral size, L , and the height, H , of the simulation domain on the apex-FEF of a single conducting ellipsoidal emitter. Firstly, we analyze the error, ε , in the calculation of the apex-FEF as a function of H and L . Importantly, our results show that the effects of H and L on ε are scale invariant, allowing one to predict ε for ratios L/h and H/h , where h is the height of the emitter. Next, we analyze the fractional change of the apex-FEF, δ , from a single emitter, γ_1 , and a pair, γ_2 . We show that small relative errors in γ_1 (i.e., $\varepsilon \approx 0.5\%$), due to the finite domain size, are sufficient to alter the functional dependence $\delta(c)$, where c is the distance from the emitters in the pair. We show that $\delta(c)$ obeys a recently proposed power law decay [R. G. Forbes, J. of Appl. Phys. **120**, 054302 (2016)] in the limit of infinite domain size ($\varepsilon = 0$, say), in contrast to a long time established exponential decay [J.-M. Bonard *et al.* Advanced Materials **13**, 184 (2001)]. Thus, power law functional dependence, $-\delta \sim c^{-n}$, with $n = 3$, is suggested to be a universal signature of the charge-blunting effect, at sufficient large distances between similar emitters with any shape. These results explain the origin of the discrepancies in the literature and improves the scientific understanding of the field electron emission theory, for accurate characterization of emitters in small clusters or arrays.

PACS numbers: 73.61.At, 74.55.+v, 79.70.+q

The emission of electrons by a conducting surface, when a strong electrostatic field is applied, is an interesting phenomenon that has led to important scientific and technological developments [1–9], specially in the particular regime of Cold Field Electron Emission (CFE) [10–16]. Recently, great attention has been given by field emission community to the research of the electrostatics behind single or small cluster of emitters [17–27], aiming to understand the emitter's interaction that leads to charge-transfer and neighbor-field effects [22]. Particularly, an important Field Emission (FE) characterization parameter is the apex-field enhancement factor (FEF) [4]. The apex-FEF, for a single emitter in a parallel-plate diode configuration, γ_1 , can be defined by,

$$\gamma_1 = E_1/E_M, \quad (1)$$

where E_1 corresponds to the local field at the apex of the single emitter and E_M the applied (macroscopic) field. In the case of a pair of identical emitters, the corresponding apex-FEF is expected to be reduced to a lower value, γ_2 , mainly due to the physical effect called charge-blunting (also known by shielding effect), which results from the requirement that the Fermi level be the same everywhere

in the emitter plate and both emitters. Thus, it is possible to define a fractional ratio $\rho \equiv \gamma_2/\gamma_1$ and a fractional change in the apex-FEF, δ , as

$$\delta \equiv \rho - 1 = \frac{\gamma_2 - \gamma_1}{\gamma_1}. \quad (2)$$

With infinite regular arrays, this fractional difference has been extensively analyzed. In a recent work [22], Forbes used floating spheres at emitter-plate potential (FSEPP) model to pointed out that discrepancies exist between the analytical results and formula previously fitted to numerical results in the literature [28, 29], based on finite element technique. These discrepancies include the functional dependence between δ and the separation between emitters. For two conducting floating spheres, Forbes showed that the fractional apex-FEF decays according as $-\delta \sim c^{-3}$, for large c , where c corresponds to the distance between the centers of the spheres [22]. These results had been confirmed recently using finite elements method for a pair of conducting identical hemispheres on cylindrical post (HCP) [25]. This suggest that the power law functional dependence $-\delta \sim c^{-3}$ may be more general and applicable to other emitters with different shapes. However, the well known Bonard *et al.* fitting formula [28], as reformulated by Jo *et al.* [29], shows that δ in a small array of hemisphere on HCP conducting emitters [28, 29] is given by

* thiagoaa@ufba.br

[†] fernando.dallagnol@ufsc.br

$$-\delta^n = \exp\{-2.3172(c/h)\}, \quad (3)$$

where h is the height of the emitters. The superscript “ n ” from hereon, shall indicate that the quantity carrying this index was determined numerically, opposed to the same variables without the index, which is determined exactly. Generalization of the Eq.(3) has been recently proposed by Harris and collaborators by using line charge model [19, 20]. The main goal of this rapid communication is to investigate the origin of the discrepancies, between analytical and numerical results, based on precise numerical solution of Laplace’s equation, by using finite elements technique, for a specified geometry. For this, we proceed as follow: (i) we determine numerically the single-emitter apex-FEF γ_1^n ; (ii) for the two-emitters, calculate δ numerically.

The apex-FEF for HCP emitters are apparently well understood, as there are many theoretical works on this subject. However, the numerical precision in γ_1^n sensibly affects δ^n , which is not well understood. Some authors using finite elements [29, 30] had reported FEF with error of $\sim 3\%$ in the range of aspect ratios $4 \leq h/r \leq 3000$ (r corresponds to the radius of the hemisphere over the cylindrical post). This error may be sufficiently small for many analyses. However, errors of this order can influence the true behavior in δ for large c , as we will discuss below. Furthermore, an analytical solution for HCP emitters is not known nor the existing formulae are particularly good to fit the whole range of aspect ratios including very low and very high values. The numerical works by Edgcombe and collaborators based in finite elements method [4, 30], Kokkorakis and collaborators simulating a HCP as a cylindrical array of touching spheres [31] and Read and Bowring based on boundary elements method [32], corroborates these comments. More recently, some works have analyzed numerically, by using finite elements, the problem of apex-FEF in single HCP emitters [33, 34]. However, detailed information about the dimensions of the domain of simulation was not given, and the issue about how close the numerical results were to the analytical ones was not answered. Thus, we investigate the electrostatics of two identical hemi-ellipsoidal emitters, where the corresponding apex-FEF is known exactly for an isolated single emitter [4]. Let r denote the semi-minor axis of the generating ellipse and h its semi-major axis, i.e., the ellipses’ radius and height are r and h , respectively (see Fig.1), and define:

$$\nu \equiv h/r \quad ; \quad \xi \equiv (\nu^2 - 1)^{1/2}. \quad (4)$$

The apex FEF of a single hemi-ellipsoid emitter is then given by [4]:

$$\gamma_1 = \frac{\xi^3}{[\{\nu \ln(\nu + \xi)\} - \xi]}. \quad (5)$$

From Eq.(4), it is clear that for $\nu \rightarrow 1$, $\xi \rightarrow 0$, the hemi-ellipsoid becomes a hemisphere, and Eq.(5) evaluates to 3, as required [4].

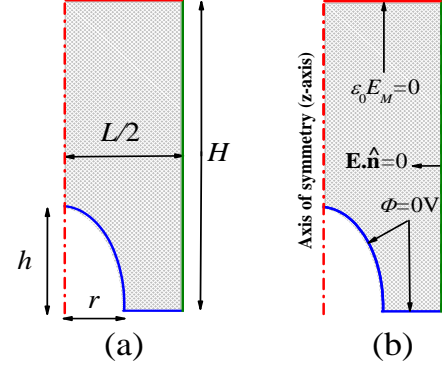


FIG. 1. Representation of simulation domain (gray color) and emitter with the corresponding dimensions indicated in (a) and the boundary conditions indicated in (b). The top boundary is a Neumann boundary condition that imposes a vertically aligned electric field as if the counter-electrode were at infinity.

When doing computer simulation based on finite elements or finite differences, there are three main sources of errors: (i) the solution converges with low precision goal; (ii) mesh is too coarse or (iii) the simulation domain does not represent the intended system accurately. In this work, we focus on the effect of the latter item. Particularly, we investigate how the size of the simulation domain affects the error, regardless of the tolerance in numerical precision or the fineness of the mesh. Simulations that involve the solution of Laplace’s equation using finite elements or finite differences require a minimum volume surrounding the region of interest. If domains are too small, the boundaries have an electrostatic effect on the emitter causing an undervaluation of the FEF. To avoid this issue, it may be possible to overestimate the size of the domain, however, this procedure may also be time and memory consuming, mainly in full three-dimensional systems. Here, ε is defined relative to the analytical values from Eq.(5), i.e.,

$$\varepsilon(\%) = \frac{|\gamma_1^n - \gamma_1|}{\gamma_1} \times 100. \quad (6)$$

Figure 1(a) represents the geometry of the physical system, and we are interested in knowing the sizes L and H to provide a desirable precision on γ_1^n . It is a two-dimensional axisymmetric system with a central ellipsoidal emitter. We assume the emitter to be perfectly conductive (no electric field penetration); hence, the interior of the emitter is removed from the simulation domain. Figure 1(b) shows the boundary conditions (BC). The emitter’s surface and the bottom surface (substrate)

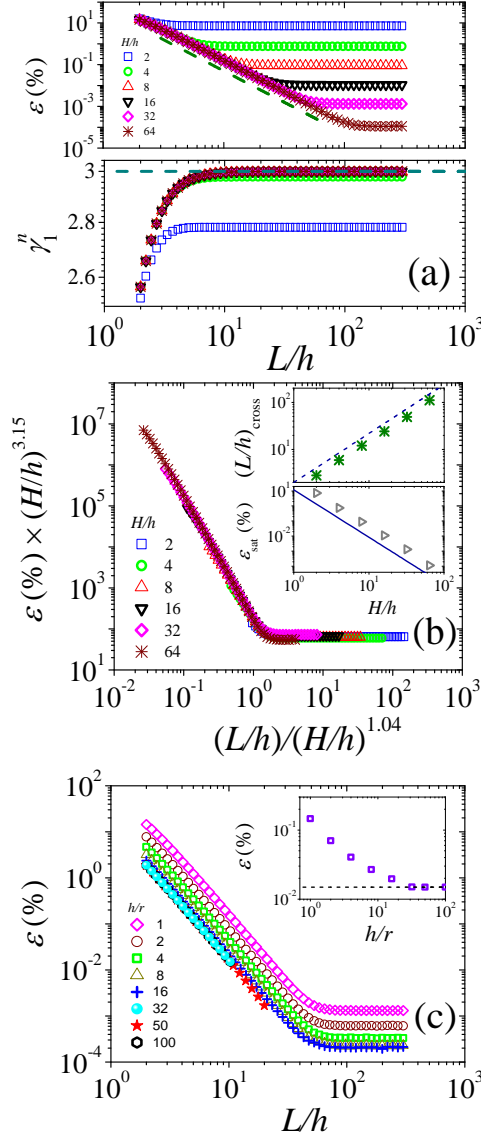


FIG. 2. (a) Error (top panel), ε [see Eq.(6)], in the apex field enhancement factor of a hemisphere ($h/r = 1$) due to the normalized size of the simulation domain L/h for various values of the H/h . The slope of the dashed line is -3 . The bottom panel shows the convergence of the numerical apex FEF toward the exact value (dashed line) for values of H/h shown in the top panel. (b) Collapse of all curves shown in (a) by replacing the variables $\varepsilon \rightarrow \varepsilon \times (H/h)^{3.15}$ and $L/h \rightarrow (L/h) \times (H/h)^{1.04}$ (see text for details). The inset (top panel) shows the crossover ratio, L/h_{cross} , estimated from (a), as a function of H/h . The dashed line has slope (1.04 ± 0.01) . The bottom panel in the inset shows the saturation error, ε_{sat} , estimated from (a), in the plateau region, as a function of H/h . The full line has slope (3.15 ± 0.03) . (c) ε as a function of L/h , for $H/h = 32$, and considering various aspect ratios. The inset shows the asymptotic decreasing of ε as the aspect ratio increases for $L/h \approx 10.3$.

are grounded (i.e., the electrical potential $\Phi=0$ V). The right hand side boundary is a symmetry line, i.e., this

BC imposes that the electric field, \mathbf{E} , is perpendicular to normal vector, $\hat{\mathbf{n}}$, from this boundary line (i.e., $\mathbf{E} \cdot \hat{\mathbf{n}}=0$) [35]. The top boundary is set as a surface charge density $\sigma = \epsilon_0 E_M$, where ϵ_0 is the permittivity of vacuum and E_M is the macroscopic electric field entering the domain, as appeared in Eq.(1). This BC assumes that the counter-electrode is at infinity, provided that H is sufficiently large. The width of the simulation domain is, as usual, $L/2$.

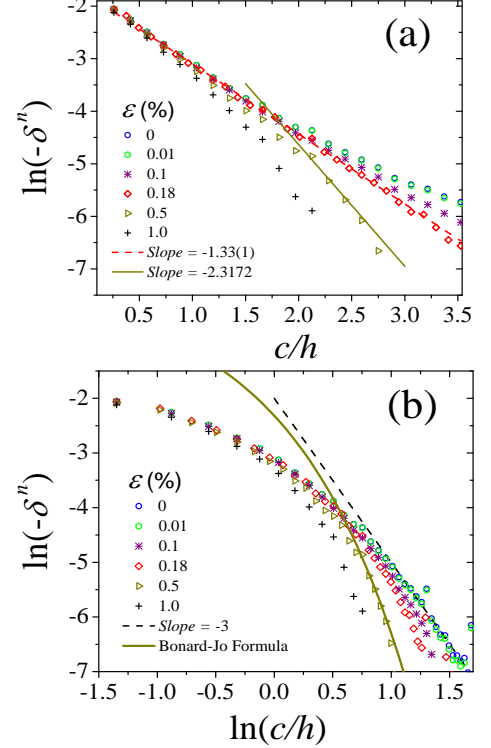


FIG. 3. Decay in $-\delta^n$ as a function of the normalized separation between the ellipsoids, c/h , for $h/r = 8$. (a) Plots \ln - \ln showing an apparent exponential decay for errors in γ_1^n of 0.18%. Slopes (-1.33 ± 0.01) (by least squares method) and -2.3172 (for comparison with Bornard-Jo results [28, 29]) are also shown; (b) Plots \ln - \ln evidencing that only errors in γ_1^n smaller than 0.01% reveals the power law with decay $-\delta^n \sim (c/h)^{-3}$. Plot of Bornard-Jo formula [see Eq.(3)] and the slope -3 are also shown. Plots corresponding to other errors up to 1% are also shown.

To calculate the FEF γ_1^n , we have used the commercial software COMSOL(version 5.3), based on the finite elements method. We want to stress that the analysis in this work is not limited to any particular method or computer code. Any method will require a minimum domain size to yield a desired precision. In our analysis, we took care to have enough numerical precision and sufficient number of mesh elements not to compromise the evaluation of ε . The ε shall be solely due to the finite size of the simulation domain. Figure 2(a) (top panel) shows ε as a function of L/h , for several ratios H/h and aspect ratio $h/r = 1$ (i.e., a hemisphere emitter as discussed

previously). It is interesting to observe (for example, for $H/h = 64$) a very clear power law behavior showing that ε scales as $\varepsilon \sim (L/h)^{-3}$ before saturation. This is a consequence of the electrostatic interactions between the emitter and its images generated by the boundaries. The exponent -3 that appears in Fig.2(a) is, in principle, not related to the trend in δ obtained by Forbes ($\delta \sim c^{-3}$) that we discussed earlier. Although there might be a possible correlation, it is not our goal to investigate this here. The bottom panel illustrates the convergence of γ_1^n towards γ_1 as the ratio L/h increases, for same values H/h shown in the top panel.

Importantly, by exploring the scaling properties of electrostatics, it is possible to collapse all curves shown in Fig.2(a) (top panel) in a single curve, as shown in Fig.2(b). A good collapse observed reflects that the effects of L and H on γ_1^n are scale invariant. The collapse of data in a single curve was obtained in three steps. First, we estimate the value of the saturation error, ε_{sat} , by the plateau region from data presented in Fig.2(a) (top panel). A clear power law behavior is observed, where $\varepsilon_{sat} \sim (H/h)^{-3.15 \pm 0.03}$. Subsequently, a crossover at $(L/h)_{cross}$, for each H/h , has been estimated by intersection between ε_{sat} and the power law decay. A nearly linear dependence $(L/h)_{cross} \sim (H/h)^{1.04 \pm 0.01}$ has been found. These two steps lead to collapse the data by replacing the variables $\varepsilon \rightarrow \varepsilon \times (H/h)^{3.15}$ and $L/h \rightarrow (L/h) \times (H/h)^{1.04}$. Thus, our results suggest that $\varepsilon/\varepsilon_{sat}$ is a function of $(L/h)/(L/h)_{cross}$ only, i.e.,

$$\varepsilon(\%) \sim \varepsilon_{sat} \mathfrak{F} \left\{ \frac{(L/h)}{(L/h)_{cross}} \right\}, \quad (7)$$

where \mathfrak{F} is a scaling function. The existence of the saturation errors, $\varepsilon_{sat} > 0$, suggests that, in addition to finite-size effects, the numerical solution converged (independent with the ratio L/h) for a given H/h . Thus, it is necessary to estimate the value of the ratio $\varepsilon(\%)/\varepsilon_{sat}$ at the plateau in Fig.2(b). With this procedure and considering the scaling given by Eq.(7), one is able to determine the error expected from numerical simulations for a given H/h . We have found (including error bars)

$$\varepsilon(\%) \approx (H/h)^{-3.15 \pm 0.03} \times (65 \pm 5). \quad (8)$$

For example, considering $H/h = 8$, Eq.(8) predicts $\varepsilon \approx 0.092\%$ that is in excellent agreement with the corresponding error shown in Fig.2(a), that is 0.089% .

Figure 2(c) shows ε as a function of L/h , for $H/h = 32$ and various aspect ratios. The results show that ε tends to decrease, in an asymptotic way, when the h/r increases. In the inset, we observe this trend, for $L/h \approx 10.3$. These results suggest that ε , for $h/r = 1$, represents the upper bound of the error so that, keeping the proportions H/h and L/h in the simulations for $h/r > 1$, ε is expected to be lower than that evaluated by using Eq.(8). Also, it is possible to observe that the error converges for $h/r \gtrsim 32$ (about one order of magnitude lower).

Next, we can evaluate the apex-FEF from a pair of identical ellipsoidal emitters, γ_2^n , to see how the error in γ_1^n relates to the trend in the δ^n . To determine δ^n , we compute γ_2^n with error $\varepsilon = 0.01\%$, using the size of the domain compatible with this error. With this error, our results show that γ_2^n can be considered analytical by comparison with γ_1^n , which we will vary. The number of mesh elements used in these analysis were $\gtrsim 3 \times 10^5$ depending on L and H and the convergence tolerance was $< 10^{-5}$. These choices are sufficient to avoid additional errors in the apex-FEFs, other than the error due to the finite domain size. The results are presented for $h/r = 8$, which are expected to be the same for higher aspect ratios, as already observed in the inset of the Fig.2(c). Figure 3 shows δ^n with different ε in the determination of γ_1^n . Here, $\varepsilon = 0$ mean that $\gamma_1^n = \gamma_1$, that is computed by Eq.(5). In Fig.3(a) $-\delta^n$ is plotted as a function of the ratio c/h , in mono-log plot, to evidence exponential behaviors as straight lines. The results indicate that the exact solution ($\varepsilon = 0$) is clearly not an exponential. However, if γ_1^n is computed with error of only 0.18% , $-\delta^n$ apparently decays exponentially with slope -1.33 ± 0.01 . The ln-ln plot in Fig.3(b) is best to review a power law decay for larger c/h . Indeed, the curve for $\varepsilon = 0$ has the slope of -3 as predicted by Forbes, using the FSEPP model [22], and by us with two HCP emitter's model [25]. These results suggest that the physics behind charge-blunting effect manifests with the power law behavior $-\delta \sim c^{-3}$ for identical emitters with any shape.

Exponential decays in $-\delta$, have also been hypothesized in the experimental works of Gröning *et al.* [36], that used carbon nanotube (CNT) thin films deposited by a plasma enhanced chemical vapor deposition process, and Cole *et al.* [37] with Large Area Field Emitters (LAFEs) formed by carbon nanofibres. Similar exponential decay rates (slopes close to -1.40 and -1.25 , respectively) were obtained within the experimental error. We observe exponential behavior with similar slope for $\varepsilon = 0.18\%$, possibly justifying Gröning's and Cole's results by the error in the γ_1 estimation (close to 500 in Fig.9(a) of the Ref.[36] and 300 in Fig.2(c) of the Ref.[37]). Similarly, Bonard *et al.* and Jo *et al.* [28, 29] have found exponential decays in $-\delta^n$ for patterned CNT films, consistent with errors in γ_1^n of the order of $\varepsilon = 0.5\%$, as shown in Fig.3(a), where slope similar to that observed by Eq.(3) (i.e., -2.3172) has been found. As a consequence, in the high c/h limit, slope larger than -3 in ln-ln plot is observed, as shown in Fig.3(b). Errors smaller than 1% can be considered good for many situations, however, to determine the asymptotic trend in $-\delta^n$, the evaluation of the apex-FEF of the emitters must be carried out with high precision ($\varepsilon \lesssim 0.01\%$, say) when the numerical and analytical results are indistinguishable, as shown in Fig.3.

In summary, we have shown the origin of the literature discrepancies in the fractional reduction of the apex-FEF, δ , considering a pair of field emitters, by using precise numerical calculations. Our results show that the effects of the domain height, H , and lateral size, L , on ε are scale

invariant. This feature allows one to predict the error on the calculation of an apex-FEF of a single tip field emitter with specified ratios L/h and H/h . This scaling relation allows one to work with a desired error for accurate study of the electrostatic effects on the fractional reduction of the apex-FEF, due to the proximity of the emitters in small clusters or arrays. Our results also suggest that the power law functional dependence, $-\delta \sim c^{-3}$, is universal for large distances between emitters, applicable to emitters with any shape and a signature of the charge-blunting effect in LAFEs. This contrasts with a long time established exponential decay, in which an apparent non-universal decay rate, as reported in the literature, seems

to be an effect of error $0.2\% \lesssim \varepsilon \lesssim 0.5\%$ in the calculation of γ_1^n . These results improve the scientific understanding of the field electron emission theory. The use of the scaling presented in Eqs.(7) and (8) is suggested in the numerical simulations for accurate comparison, characterization and understanding of the physics behind real emitters in clusters or arrays.

TAdA acknowledges Royal Society under Newton Mobility Grant, Ref: NII60031. TAdA thanks Richard Forbes for illuminating discussions during a scientific visit to University of Surrey (U.K.), where this work was motivated.

-
- [1] E. W. Müller, *Zeitschrift für Physik* **106**, 541 (1937).
 - [2] E. W. Müller, *Zeitschrift für Physik* **131**, 136 (1951).
 - [3] E. W. Müller and K. Bahadur, *Phys. Rev.* **102**, 624 (1956).
 - [4] R. G. Forbes, C. Edgcombe, and U. Valdrè, *Ultramicroscopy* **95**, 57 (2003).
 - [5] M. T. Cole, M. Mann, K. B. Teo, and W. I. Milne, in *Emerging Nanotechnologies for Manufacturing (Second Edition)*, Micro and Nano Technologies, edited by W. Ahmed, and M. J. Jackson (William Andrew Publishing, Boston, 2015) second edition ed., pp. 125 – 186.
 - [6] F. Djurabekova, S. Parviainen, A. Pohjonen, and K. Nordlund, *Phys. Rev. E* **83**, 026704 (2011).
 - [7] S.-D. Liang and L. Chen, *Phys. Rev. Lett.* **101**, 027602 (2008).
 - [8] A. Pascale-Hamri, S. Perisanu, A. Derouet, C. Journet, P. Vincent, A. Ayari, and S. T. Purcell, *Phys. Rev. Lett.* **112**, 126805 (2014).
 - [9] H. Cabrera, D. A. Zanin, L. G. De Pietro, T. Michaels, P. Thalmann, U. Ramsperger, A. Vindigni, D. Pescia, A. Kyritsakis, J. P. Xanthakis, F. Li, and A. Abanov, *Phys. Rev. B* **87**, 115436 (2013).
 - [10] H. Jeffreys, *Proceedings of the London Mathematical Society* **s2-23**, 428 (1925).
 - [11] R. H. Fowler and L. Nordheim, *Proceedings of the Royal Society of London A: Mathematical, Physical and Engineering Sciences* **119**, 173 (1928).
 - [12] R. E. Burgess, H. Kroemer, and J. M. Houston, *Phys. Rev.* **90**, 515 (1953).
 - [13] E. L. Murphy and R. H. Good, *Phys. Rev.* **102**, 1464 (1956).
 - [14] R. G. Forbes and J. H. Deane, *Proceedings of the Royal Society of London A: Mathematical, Physical and Engineering Sciences* **463**, 2907 (2007).
 - [15] J. H. B. Deane and R. G. Forbes, *Journal of Physics A: Mathematical and Theoretical* **41**, 395301 (2008).
 - [16] R. G. Forbes, *Proceedings of the Royal Society of London A: Mathematical, Physical and Engineering Sciences* **469**, 20130271 (2013).
 - [17] J. R. Harris, K. L. Jensen, and D. A. Shiffler, *Journal of Physics D: Applied Physics* **48**, 385203 (2015).
 - [18] J. R. Harris, K. L. Jensen, D. A. Shiffler, and J. J. Petillo, *Applied Physics Letters* **106**, 201603 (2015).
 - [19] J. R. Harris, K. L. Jensen, and D. A. Shiffler, *AIP Advances* **5**, 087182 (2015).
 - [20] J. R. Harris, K. L. Jensen, W. Tang, and D. A. Shiffler, *Journal of Vacuum Science & Technology B, Nanotechnology and Microelectronics: Materials, Processing, Measurement, and Phenomena* **34**, 041215 (2016).
 - [21] W. W. Tang, D. A. Shiffler, J. R. Harris, K. L. Jensen, K. Golby, M. LaCour, and T. Knowles, *AIP Advances* **6**, 095007 (2016).
 - [22] R. G. Forbes, *Journal of Applied Physics* **120**, 054302 (2016).
 - [23] T. A. de Assis and F. F. Dall’Agnol, *Nanotechnology* **27**, 44LT01 (2016).
 - [24] T. A. de Assis and F. F. Dall’Agnol, *Journal of Applied Physics* **121**, 014503 (2017).
 - [25] F. F. Dall’Agnol, T. A. de Assis, and R. G. Forbes, in *30th International Vacuum Nanoelectronics Conference (IVNC)* (2017) pp. 230–231.
 - [26] F. F. Dall’Agnol and T. A. de Assis, *Journal of Physics: Condensed Matter* **29**, 40LT01 (2017).
 - [27] J. R. Harris, K. L. Jensen, J. J. Petillo, S. Maestas, W. Tang, and D. A. Shiffler, *Journal of Applied Physics* **121**, 203303 (2017).
 - [28] J.-M. Bonard, N. Weiss, H. Kind, T. Stöckli, L. Forró, K. Kern, and A. Châtelain, *Advanced Materials* **13**, 184 (2001).
 - [29] S. H. Jo, Y. Tu, Z. P. Huang, D. L. Carnahan, D. Z. Wang, and Z. F. Ren, *Applied Physics Letters* **82**, 3520 (2003).
 - [30] C. J. Edgcombe and U. Valdrè, *Journal of Microscopy* **203**, 188 (2001).
 - [31] G. C. Kokkorakis, A. Modinos, and J. P. Xanthakis, *Journal of Applied Physics* **91**, 4580 (2002).
 - [32] F. Read and N. Bowring, *Nuclear Instruments and Methods in Physics Research Section A: Accelerators, Spectrometers, Detectors and Associated Equipment* **519**, 305 (2004), proceedings of the Sixth International Conference on Charged Particle Optics.
 - [33] W. Zeng, G. Fang, N. Liu, L. Yuan, X. Yang, S. Guo, D. Wang, Z. Liu, and X. Zhao, *Diamond and Related Materials* **18**, 1381 (2009).
 - [34] D. Roveri, G. Sant’Anna, H. Bertan, J. Mologni, M. Alves, and E. Braga, *Ultramicroscopy* **160**, 247 (2016).
 - [35] F. F. Dall’Agnol and D. den Engelsen, *Nanoscience and Nanotechnology Letters* **5** (2013).
 - [36] O. Gröning, O. M. Küttel, C. Emmenegger, P. Gröning,

and L. Schlapbach, Journal of Vacuum Science & Technology B: Microelectronics and Nanometer Structures Processing, Measurement, and Phenomena **18**, 665 (2000).

[37] M. Cole, K. B. K. Teo, O. Groening, L. Gangloff, P. Legagneux, and W. I. Milne, Sci. Rep. **4**, 4840 (2014).